Precise Stellar Radial Velocities
ASP Conference Series, Vol. 185, 1999
J. B. Hearnshaw and C. D. Scarfe, eds.

The Advanced Fiber-optic Echelle (AFOE) and Extrasolar Planet Searches

P. Nisenson, A. Contos, S. Korzennik, and R. Noyes

Harvard-Smithsonian Center for Astrophysics, Cambridge, MA 02138

T. Brown

High Altitude Observatory, CO 80307

Abstract.
The Advanced Fiber-Optic Echelle (AFOE) is a fiber-fed bench-top spectrograph specifically designed for precise radial velocity observations. The AFOE is permanently located at the 1.5-m telescope at Smithsonian's Whipple Observatory in Arizona and is regularly used for monitoring exo-planet candidate stars and for asteroseismology observations. In this paper, we discuss the status of the instrument, as well as an upgrade to the instrument, a Fabry-Perot reference, which may prove important both for the AFOE and for all precise radial velocity (PRV) facilities.

1. Introduction

The Advanced Fiber-Optic Echelle (AFOE) (Brown *et al* 1994) is a fiber-fed bench-top spectrograph specifically designed for precise radial velocity observations. The spectrograph is located in a temperature controlled room on an isolated optical table. The signals are fed into the spectrograph using either straight-through fibers for higher throughput or double-scrambled fibers for the highest precision required by stellar seismology. Two means of providing a stable reference are implemented: spectral orders from a ThAr hollow cathode lamp are interlaced with the stellar orders on the CCD detector, and an iodine (I2) cell may be inserted in the beam at the telescope interface. The AFOE had two major scientific justifications for its construction: detection of extra-solar planets and asteroseismology, and it was also viewed as a potential prototype for ground-based PRV observational instruments. Since seeing first light in the fall of 1993, the AFOE has undergone many changes and our understanding of both hardware and software issues for PRV has greatly improved. In this paper, we update the description of the AFOE with its many improvements since 1993; we discuss the new reference system based on a stabilized Fabry-Perot interferometer which we are developing; and we will show some results from our exo-planet detection program.

https://doi.org/10.1017/S025292110004848X Published online by Cambridge University Press

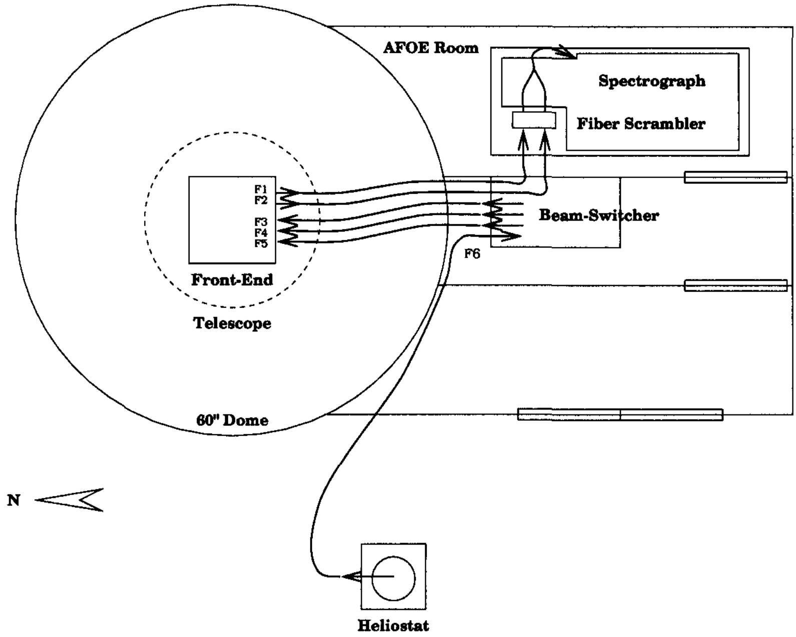

Figure 1. Layout for the AFOE at the Whipple Observatory 1.5-m telescope

2. The AFOE Layout

Figure 1 shows the general layout for the AFOE. There are three major components to the system: the front-end, the beam-switcher, and the spectrograph. The front-end is mounted to the Whipple observatory 1.5 meter telescope at its cassegrain focus. It is optically connected to the beam switcher and the spectrograph through fiber optic cables, a little over 10 meters from the front end to the beam-switcher and 15 meters to the spectrograph. It is also automated and computer controlled over an ethernet link. The beam-switcher provides white light for flat-fielding and ThAr as a reference source to the front-end. The three pickup fiber optic cables going from the beam switcher to the front end are 300 μm diameter, while the fibers which bring the stellar signal and the references to the spectrograph have a 200-μm core diameter. The projected size of the fiber on the sky is approximately 2.7 arc seconds. The AFOE also has a small telescope mount with a fiber mounted to it that can be used for feeding sunlight into the beam-switcher. Sunlight can be fed into the front end and then into the spectrograph as a test source for system stability and for comparison with asteroseismology results.

https://doi.org/10.1017/S025292110004848X Published online by Cambridge University Press

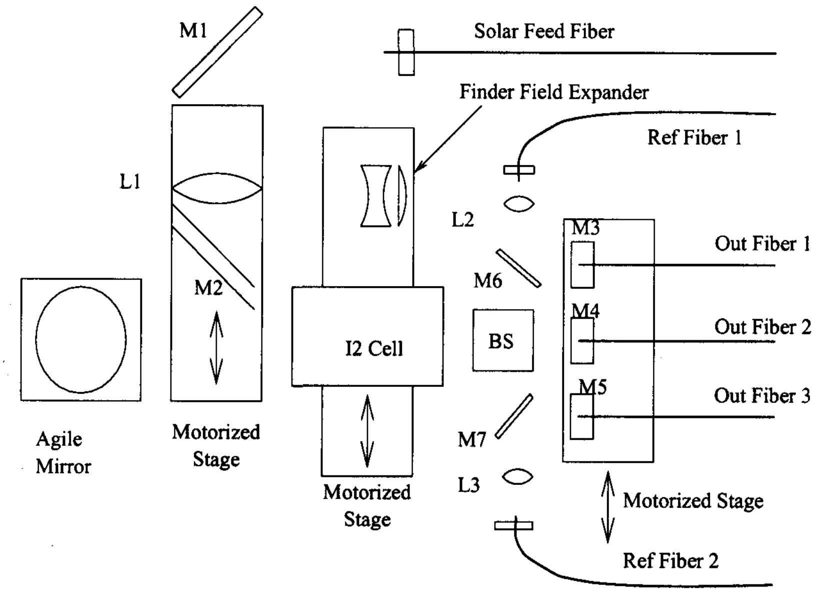

Figure 2. Front end layout

3. The Front End

The AFOE front end is the interface to the telescope, accepting starlight and the reference sources and feeding that light through fibers to the spectrograph. Figure 2 shows a layout of the front end. The telescope beam reflects off an agile mirror feeding light into the system in a plane parallel to the telescope back plate. The agile mirror is driven by speaker coils and has a resonance at about 13 Hz, allowing us to actively guide the focussed beam at about a 2 Hz rate. A signal from a TV guide camera is used to compute an error signal which then controls the mirror. The beam is focused onto the pickup fibers, either through an I2 absorption cell or directly. The I2 cell is mounted on a motorized stage which allows one to move the cell in or out of the beam and also to insert a demagnifying lens which widens the field of the TV guide camera (to about 3 arcminutes). A beamsplitter (BS) picks off 4 % of the incoming light and sends it to a Pulnix CCD camera for guiding. The pickup fibers are mounted on a motorized stage, allowing one to select which of three fibers has the stellar beam and which the reference light. One of the pickup fibers (m1) goes directly to the slit of the spectrograph, while the other two fibers go to a fiber-scrambler on the spectrograph table. We select two of the three fibers for signal and reference.

Reference light is brought into the front end on three fibers. One of the reference fibers is labeled Solar Feed and it is introduced into the system by moving a lens (L1) and mirror (M2) into the optical path with a motorized stage. It can bring in either sunlight from our solar feed telescope or reference light. Lens L1 is chosen so that the focal ratio of the beam matches the focal ratio of the telescope (f/10). The beam switcher (see below) allows selection of either a tungsten source (for flat fields) or the ThAr hollow cathode source as a wavelength reference and feeds that light into the reference fibers. Reference fibers 1 and 2, coming from the beam switcher, are also reimaged with an f/10 cone onto the pickup fibers.

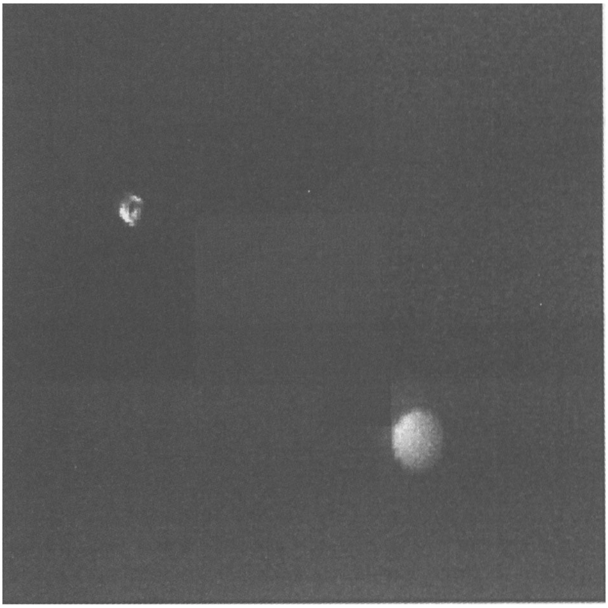

Figure 3. TV guider display

The pickup fibers are mounted in 6-mm diameter ferrules (which are held in adjustable fiber positioners) whose faces have been beveled to 45 degrees and then polished. The reflected light from the ferrule which is in the system on-axis position (where the stellar light comes in) reflects that light into a periscope arrangement which produces a demagnified image of the ferrule face and the fiber in a corner of the guide TV camera. This image is used as a check that the light is being correctly guided into the fiber. Figure 3 shows the TV display, with the image on the fiber in the upper left and the direct image (from the beam splitter) in the lower right. The image is frame grabbed and we select only the

https://doi.org/10.1017/S025292110004848X Published online by Cambridge University Press

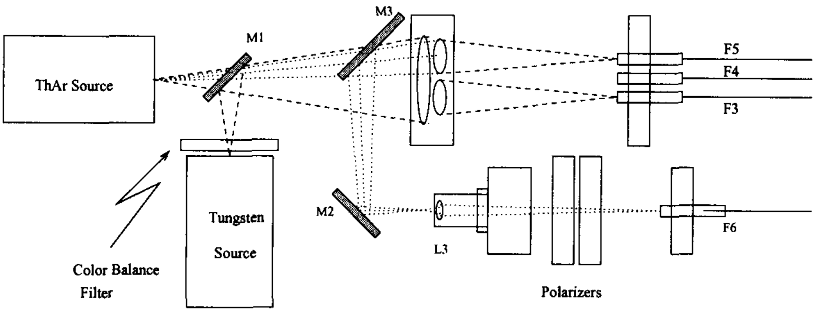

Figure 4. Diagram of the beam switcher

region around the direct image for estimating the star position and feeding back to the agile mirror.

4. The Beam Switcher

The beam-switcher shown in Figure 4 is setup on a separate, accessible table. Its purpose is to feed various reference sources through fibers into the front-end. Computer controlled mirrors select between a ThAr hollow cathode lamp, a tungsten lamp, or a fiber which brings in light from the Solar Feed. In the current mode of operation, the ThAr reference is used during all stellar (or solar) observing. The tungsten lamp is filtered to flatten its spectrum and used for generating either flats for flat-fielding the stellar data, or with the I2 reference cell, for producing I2 flats needed for the I2 data reduction. One other option provided by the beam-switcher is that it allows sunlight to be brought in with a fiber which is mounted outside the dome on a solar tracking mount, bringing solar light in for testing the precision and stability of the AFOE.

5. The Spectrograph

The light from the ThAr lamp is relayed to the front-end and then relayed to the spectrograph through a fiber which is adjacent to the stellar signal fiber. The three pickup fibers from the front-end then go to the slit of the spectrograph (two of them are relayed through a fiber-scrambler), placing a ThAr spectrum adjacent to the stellar spectrum on the CCD. The slit width is computer adjustable, allowing selection of spectral resolution. The spectrograph is built on an air-isolated optical table and is diagrammed in Figure 5. The output of the slit is collimated with an off-axis section of a Zerodur 1200 mm focal length paraboloid. The échelle is a Milton Roy 59 lines/mm grating blazed for use at 63.5 deg ($R = 2$) which has been replicated on a Zerodur substrate. The cross-disperser is a Milton Roy 150 lines/mm grating blazed for operation at 500 nm in first order. Both gratings are mounted to be computer adjustable so that,

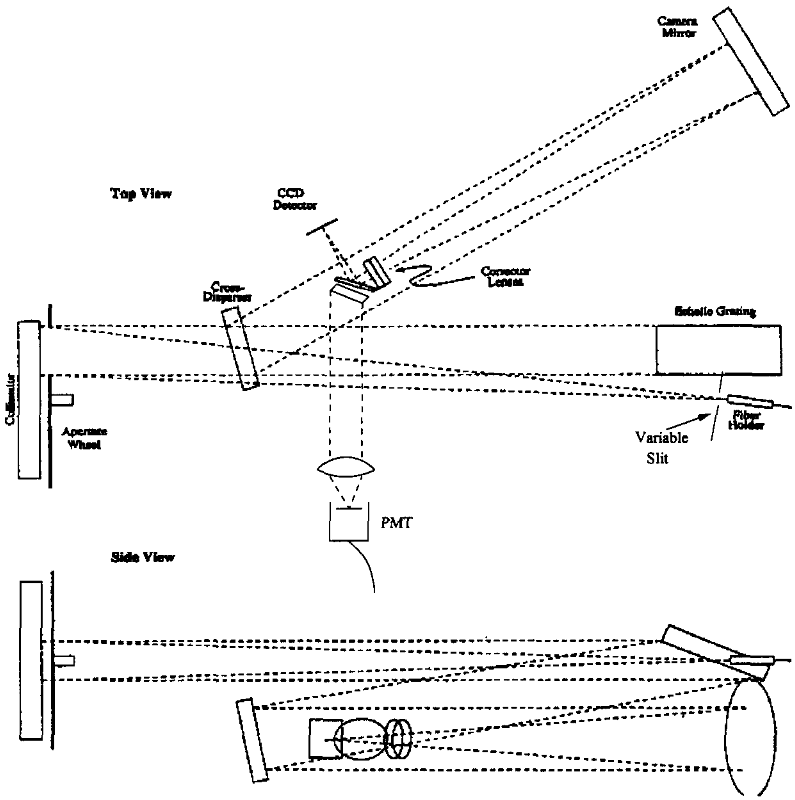

Figure 5. Spectrograph layout

for planet detection, the spectrum is always located in the same spot on the CCD. The adjustment allows selection of other spectral regions, though for our standard operation, the spectral range is kept constant at approximately 380 nm to 700 nm. The spectrograph camera is a modified Rosin design which is described in detail in Brown *et al* (1994). It is a compact design that produces images with a PSF less than 15 μm (the CCD pixel size) over the whole CCD field. A small pickoff mirror is located in the central obscuration of the Rosin camera, and this mirror feeds a photon-counting photometer that allows one to monitor the exposure level and determine precisely the temporal centroid of each exposure.

The CCD is a 2048 $\times$ 2048-pixel Loral chip that has been thinned and AR coated by Mike Lesser of Steward Observatory. It is mounted in a LN2 dewar on a specially designed stabilized mount and operates using a controller built by John Geary of SAO. The chip uses two readout amplifiers and the read time is 16 seconds, binned down to 1k $\times$ 2k. This rapid read is important for asteroseismology where cadences of as fast as 1 minute are used and maximizing the duty cycle is critical.

The spectrograph is enclosed in a PID controlled thermal environment. The spectrograph is covered and raised to a temperature a few degrees higher than ambient. The whole optical table is then enclosed in a polyethylene tent. Finally the room in which the spectograph sits is controlled in temperature to less than one degree. This level of thermal control has been found essential; otherwise the spectrum may wander by several pixels on the CCD over a night. We believe the wander is caused by differential bending of the optical table due to nonuniformity of the thermal environment in the room, but adding the tent has greatly reduced this effect.

6. I2 Data Analysis

Currently we use data taken with the I2 cell in place for all of our exo-planet detection observations. The following is a summary of our approach to determining velocities from the I2 data:

- Model the data using a spectrum of the star without I2, an FTS-scanned I2 spectrum, a parameterized representation of the wavelength solution matching the I2 wavelength scale, a model for the PSF, and additional parameters to handle scattered light, gain, etc.
- Allow the PSF to vary in a parameterized way along the dispersion direction.
- Adjust the model parameters to best match the observations in the least-squares sense.
- Obtain the line-of-sight velocity from the parameterization of the Doppler shift.
- Carry out the modeling independently for each of the six I2 spectral orders and use the scatter from the mean as an estimate of the uncertainty in the velocity.

7. The New Fabry-Perot Reference (FPR)

Each of the two techniques used to provide the precision and stability in AFOE radial velocity measurements has important limitations. Using the ThAr lamp covers the entire wavelength range of the spectrograph and provides good short term stability. However, the ThAr lamps age, so line ratios change with time, plus there are many blends and lines with good SNR are irregularly spaced. In addition, the ThAr takes up space on the detector which might otherwise be used for stellar signal and it does not have a true common path with the stellar light. The I2 cell has the advantage that it imposes its absorption lines at the beginning of the optical train, so the reference and the signal follow exactly the same optical path. I2 provides very good long term stability. However, it only covers the spectral range between 5000 Å and 6000 Å.

HAO and SAO have developed a new reference approach which takes advantage of a stabilized Queensgate Fabry-Perot interferometer, used in reflection.

https://doi.org/10.1017/S025292110004848X Published online by Cambridge University Press

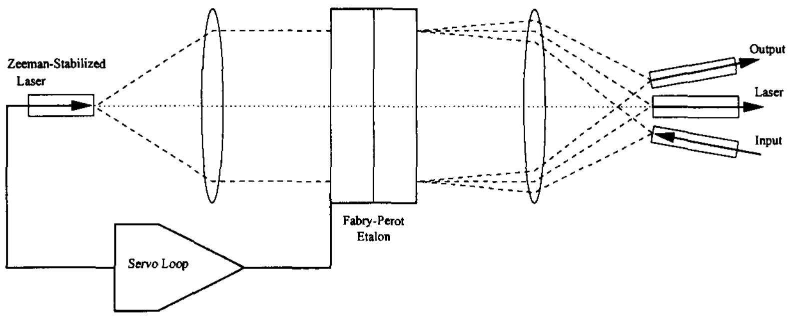

Figure 6. Front end layout

Figure 6 is a diagram of the FPR. Light from a Zeeman-stabilized laser is fed into the Fabry-Perot on one side using a fiber and a collimating objective. On the other side of the Fabry-Perot, a second object focuses the laser light onto the center fiber of three pickup fibers and this signal is fed to a photometer and the measured signal used to feedback to the active controls in the Queensgate via a computer which sets the PID of the control loop. The stellar signal is brought in on one of the outer fibers, collimated by the objective, reflected off the Fabry-Perot, and picked up by the other outer fiber. This signal then goes to the spectrograph, with evenly spaced absorption features impressed on it. The plate spacing of the Fabry-Perot sets the separation of the absorption lines, and the coatings set the line width.

Figure 7 shows some initial tests of the FPR made at HAO by feeding sunlight into the FPR and using a relatively low resolution spectrograph. The upper figure shows the spectral region which includes the NaD lines, without the FPR. The middle panel shows the FPR absorption lines using a tungsten lamp as the source (the line spacing is 0.83 Å). Any irregularity in the display is due to the CCD, which was not flat fielded. The bottom panel shows the solar spectrum with the FPR absorption features impressed on it. The current throughput of the FPR is about 50 %. We expect that optimizing coatings should increase that throughput to close to 70 %. The FPR could provide a substantial increase in the sensitivity of the AFOE since it will allow us to use the full spectral range (3800 Å to 7000 Å) and it will also let us reclaim the area on the CCD now taken up by ThAr if we replace the cross-dispersion grating to put more of the spectrum on the CCD.

8. Results

Asteroseismology results from the AFOE are shown in the paper by Brown (1999) in this volume. Results on ρ Coronae Borealis were published by Noyes *et al* (1997) and updates on those results are given by Noyes *et al* (1999). We are currently monitoring over 100 candidatecd /dol6/iau170/papers stars searching for new companions, with our observing list honed to minimize overlap with

https://doi.org/10.1017/S025292110004848X Published online by Cambridge University Press

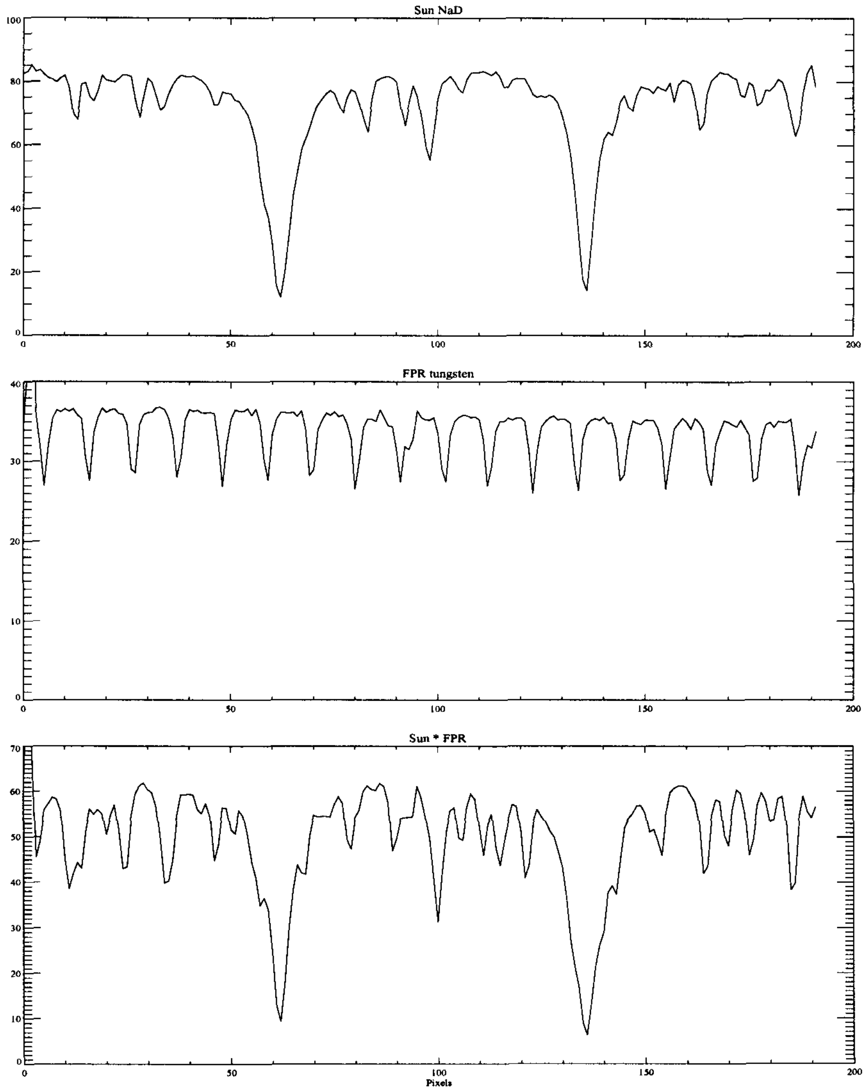

Figure 7. FPR test results: top panel – solar Na D lines; middle panel – tungsten source with FPR absorption features; bottom panel – solar Na D lines through the FPR

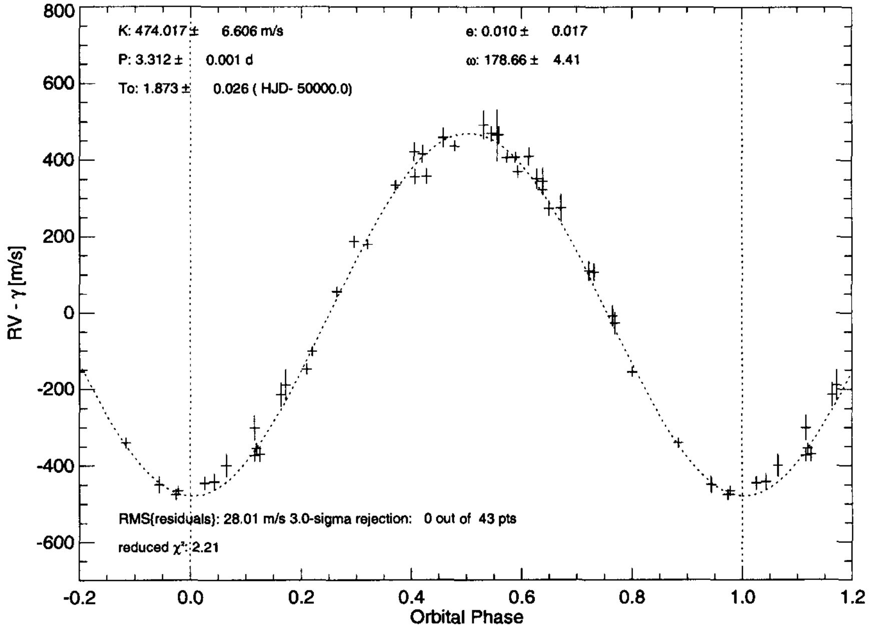

Figure 8. Fit to AFOE τ Boo radial velocities

other PRV groups. We add to this list as we reduce the number of observations on stars which show no short term variations. We are also monitoring many of the stars with known companions to possibly detect small, long-term variations which could indicate additional components of the system. As an example of AFOE radial velocities, Figure 8 shows the results from our observations of τ Boo. The large rms (28 m/s) is due to known stellar instability in τ Boo.

Discussion

Kürster: What is the wavelength spacing that you expect to use for the absorption lines of the new Fabbry-Perot wavelength reference?

Nisenson: The line spacing for the FPR is $\sim$ 1 Å (30 pixels).

Ramsey: Is there a reason that you use an autofill liquid N_2 technique rather than a closed cycle cooler?

Nisenson: We have found that filling only disturbs the detector for about 1 hr. Then it returns to a precise position. We fill in the morning, then the spectrograph is fully stable by midday.

References

Brown, T.M 1999, Proceedings of IAU Colloquium 170

Brown, T.M., Noyes, R.W., Nisenson, P., Korzennik, S.G., Horner, S 1994, PASP, **106**, 1285

Noyes, R., Jha, S., Korzennik, S., Krockenberger, M., Nisenson, P., Brown, T., Kennelly, E. and Horner, S 1997, Ap. J, 483, L111

Noyes, R.W., Contos, A.R., Korzennik, S.G., Nisenson, P., Brown, T.M., Horner, S.D 1999, Proceedings of IAU Colloquium 170

https://doi.org/10.1017/S025292110004848X Published online by Cambridge University Press